Supporting Information

Catalytic Thiophene Oxidation by Groups 4 and 5 Framework-Substituted Zeolites with Hydrogen Peroxide: Mechanistic and Spectroscopic Evidence for the Effects of Metal Lewis Acidity and Solvent Lewis Basicity

Daniel T. Bregante, Ami Y. Patel, Alayna M. Johnson, and David W. Flaherty*

Department of Chemical and Biomolecular Engineering
University of Illinois Urbana-Champaign, Urbana, IL 61801

*Corresponding Author

Phone: (217) 244-2816

Email: dwflhrty@illinois.edu

S1.0 Additional Catalyst Characterization and the Absence of Mass-Transfer Restrictions

S1.1 Catalyst Characterization

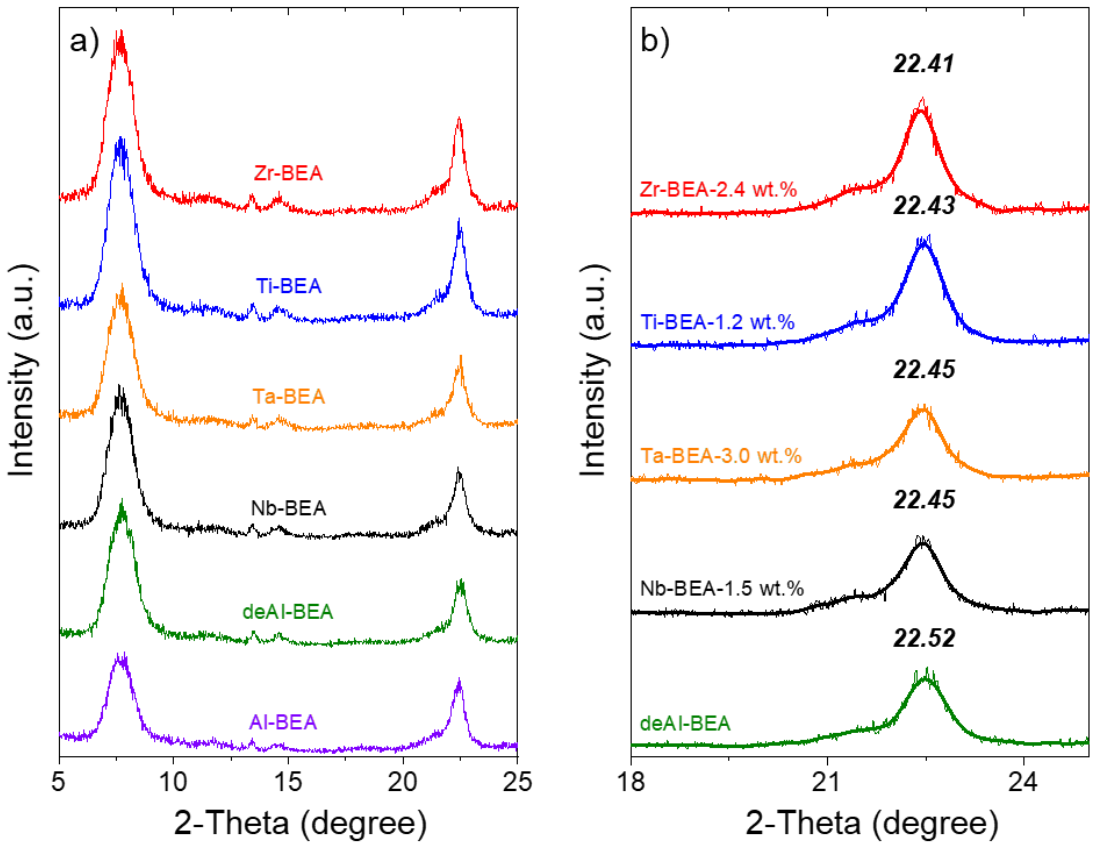

Figure S1. X-ray diffractograms for (a) Zr-BEA, Ti-BEA, Ta-BEA, Nb-BEA, dealuminated *BEA, and Al-BEA (i.e., the parent *BEA) used in the kinetic studies (Section 3 of the main text) and (B) of Zr-BEA, Ti-BEA, Nb-BEA, Ta-BEA, with weight loadings of 2.4, 1.2, 3.0, and 1.5 wt.%, respectively, and dealuminated BEA* to visualize changes in the peak position of the ~22.5 degree X-ray diffractogram feature. Bold solid lines in (b) represent a finite fourier transform to smooth the data with 10 points of fitting.

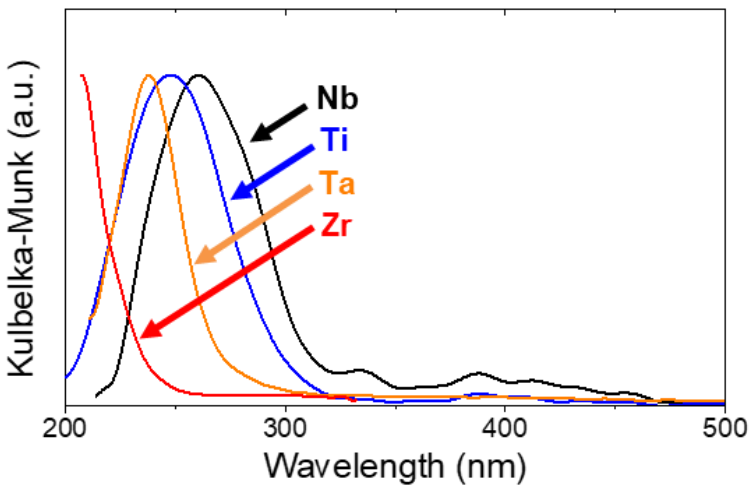

Figure S2. Normalized diffuse reflectance UV-vis spectra of Ti- (blue), Nb- (black), Ta- (orange), and Zr- (red) BEA materials diluted in a 1:10 by weight ratio with MgO. Pure MgO was used as the background. Spectral artifacts at >325 nm for Ti- and Nb-BEA arise from smoothing with a finite fourier transform with 10 points of smoothing.

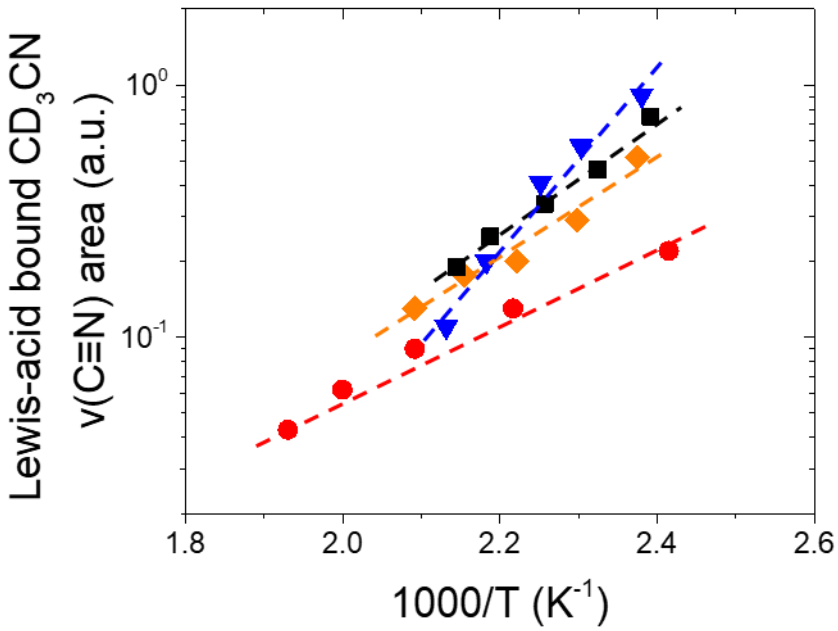

Figure S3. IR feature areas for Lewis-acid bound CD_3CN on Ti-BEA (blue ▼, 2302 cm^{-1}), Nb-BEA (black ■, 2306 cm^{-1}), Ta-BEA (orange ♦, 2312 cm^{-1}), and Zr-BEA (red ●, 2296 cm^{-1}) as a function of inverse temperature (1.5 kPa CD_3CN, 100 kPa He, 50 cm^3 min^{-1}) after background subtraction. Dashed lines represent linear fits, whose slopes are proportional to the value of ΔH_{CD3CN}.

S1.2 Experimental Verification for the Absence of Mass-Transfer Restrictions

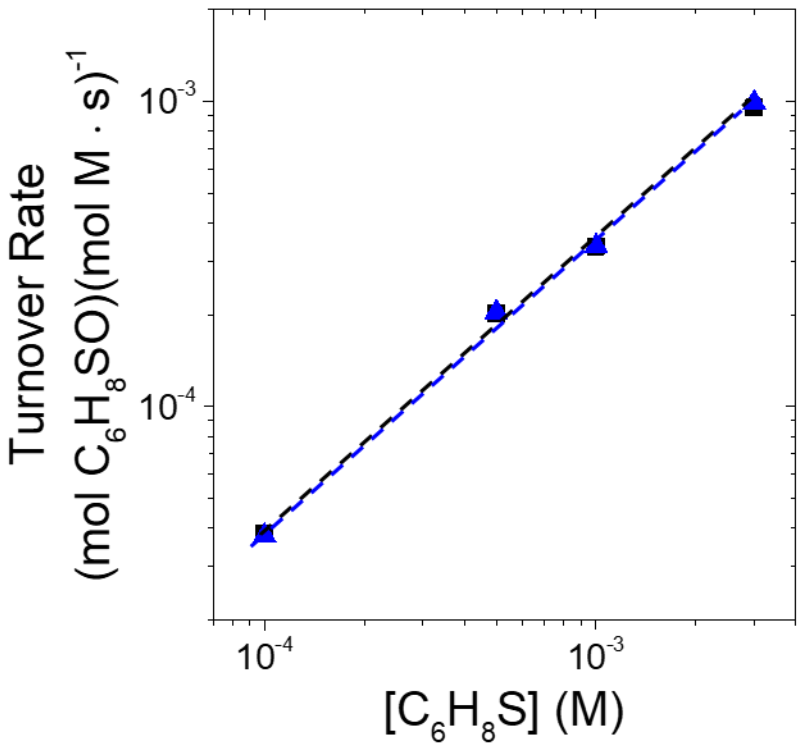

Figure S4. Turnover rates for the formation of C_6H_8SO measured as a function of [C_6H_8S] on Ti-BEA (blue solid ▲, 0.141 wt.% Ti, used in kinetics experiments in main text; 0.01 M H_2O_2, 313 K) and Ti-BEA (black ■, 0.019 wt.% Ti; 0.01 M H_2O_2, 313 K). Dashed lines are intended to guide the eye.

Figure S5 shows rates for the formation of 2,5-dimethylthiophene oxide (C_6H_8SO) measured as a function of C_6H_8S concentration for multiple metal loadings of Ti (0.141 wt.% and 0.019 wt.%) in Ti-BEA. The rate of C_8H_8O formation is invariant with metal loading, which indicates that the Madon-Boudart criterion is satisfied for Ti-BEA.[1]

In Fig. 3 (main text), C_6H_8SO formation rates are highest for Ti-BEA (of all M-BEA and M-SiO_2) under these conditions, which suggests that satisfaction of the Madon-Boudart criterion for Ti-BEA implies that the other M-BEA (i.e., those with lower turnover rates and similar crystallite size) do not possess mass-transfer restrictions.

S2. Sample Raw UV-Vis Spectrum and Spectral Processing

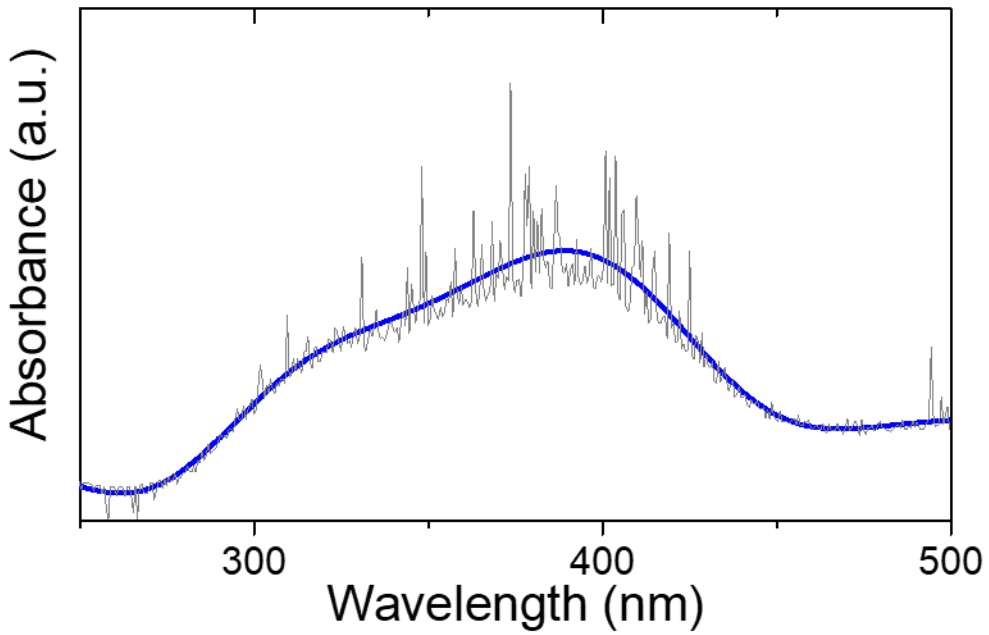

Figure S5. UV-vis absorbance spectrum (raw data, gray) of H_2O_2-treated Ti-BEA at 313 K in flowing CH_3CN (0.4 M H_2O, 0.01 M H_2O_2, 313 K) and smoothed data (bold blue line) using a finite fourier transform with 40 points of fitting performed in OriginPro®.

For all UV-vis experiments, spectra were collected at steady state (i.e., where the UV-vis features were unchanging with time) and smoothed using OriginPro® in a systematic fashion (i.e., using the same wavelength intervals and number of smoothing points).

S4. Product Selectivities over M-BEA

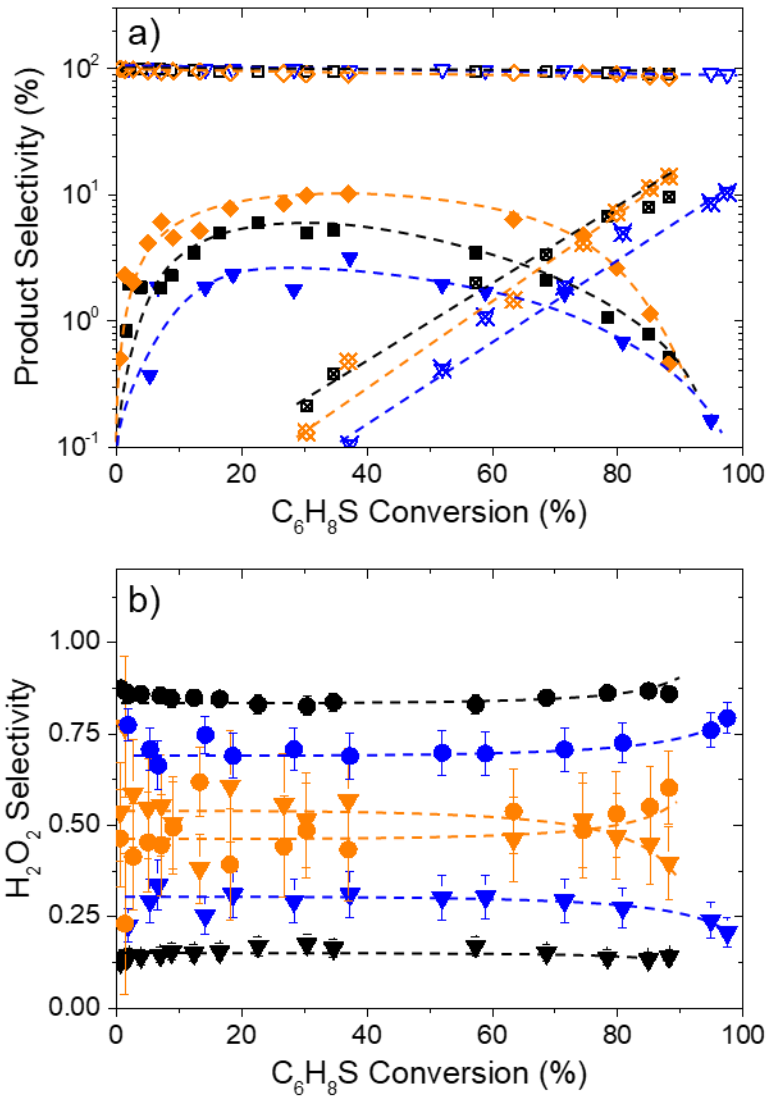

Figure S6. (a) Product selectivity towards C_6H_8SO (open symbols), $C_6H_8SO_2$ (closed symbols), and $C_6H_8SO_3$ (symbols with a "X") over Ti-BEA (blue ▼), Nb-BEA (black ■), and Ta-BEA (orange ♦) and (b) H_2O_2 selectivity towards oxidation (▼) and H_2O_2 decomposition (●) as a function of C_6H_8S conversion (5 mM C_6H_8S, 0.05 H_2O_2, 313 K) over Ti-BEA (blue), Nb-BEA (black), and Ta-BEA (orange). Dashed curves are intended to guide the eye.

S5 Supplemental Information for the Derivation of Rate Expression for Sulfoxidation and Transition State Theory

S5.1 Pseudo Steady State Hypothesis Applied to M-(O_2) Intermediates

The pseudo steady state hypothesis (PSSH) assumes that the concentration (or number) of a specific reactive species is unchanging with time during a reaction. Application of the PSSH to M-(O_2) intermediates in section 3.3, results in the following expression:

$$\frac{d[M-(O_2)]}{dt} \approx 0 = k_3[H_2O_2\ *] - k_4[C_6H_8S][M-(O_2)] + k_5[H_2O_2][M-(O_2)] + k_7[C_6H_8SO][M-(O_2)] \quad \text{(S1)}$$

where k_x represents the rate constant for step *x*, [M-(O_2)] is the number of M-(O_2) intermediates, [H_2O_2*] is the number of H_2O_2 molecules bound to active sites, and all other species within brackets ([]) are the corresponding liquid-phase concentrations. When H_2O_2 adsorption is assumed to be quasi-equilibrated (step 2, Scheme 1), equation S1 can be rearranged to yield:

$$[M-(O_2)] = \frac{k_3K_2[H_2O_2][*]}{k_4[C_6H_8S]+k_5[H_2O_2]+k_7[C_6H_8SO]} \quad \text{(S2)}$$

where [*] is the number of unoccupied (or solvent-covered) active sites. Equation S2 is then combined with equation 1 (main text) to yield equation 2 from the main text.

S5.2 Transition State Theory for Measurement of Activation Enthalpies and Entropies

Application of TST assumes that the state immediately preceding the transition state and the transition state are in equilibrium [2], which takes the form of

$$M-(O_2)+H_2O_2 \overset{K^{\ddagger}_{Dec}}{\rightleftharpoons} M-(O_2)-H_2O_2{}^{\ddagger} \tag{S3}$$

where M-(O_2)-$H_2O_2{}^{\ddagger}$ and $K^{\ddagger}_{Dec}$ represent the transition states and transition state equilibrium constants for H_2O_2 decomposition, respectively. The rates for H_2O_2 decomposition can then be expressed in terms of the numbers of transition states, resulting in

$$\frac{r_{Dec}}{[L]} = \frac{k_b T}{h}[M-(O_2)-H_2O_2{}^{\ddagger}] \tag{S4}$$

where T is the absolute temperature in Kelvin and k_b and h are Boltzmann's and Planck's constants, respectively. Measurement of the reaction rates under a M-(O_2) MASI allows equation 2 to be re-expressed as

$$\frac{r_{Dec}}{[L]} = \frac{k_b T}{h} K^{\ddagger}_{Dec}[H_2O_2] \tag{S5}$$

which allows for $K^{\ddagger}_{Dec}$ to be determined by measurement of turnover rates for each reaction pathway at a given temperature.

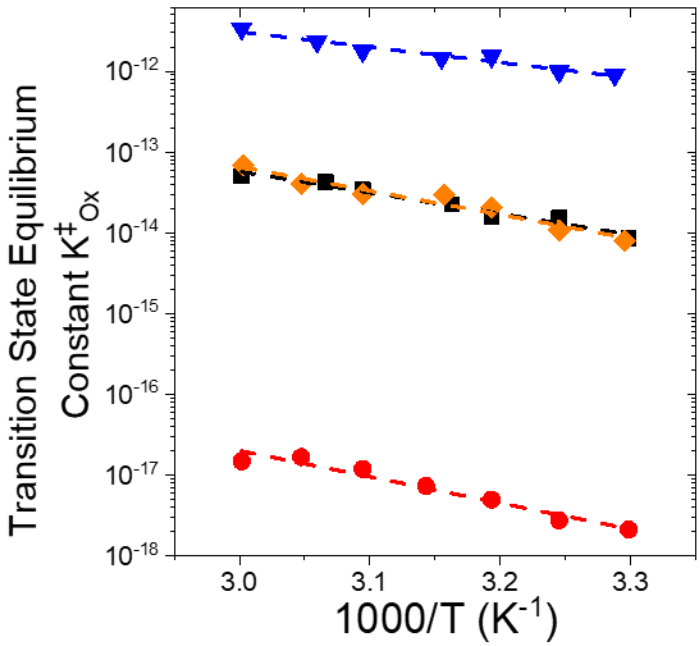

Figure S7. Transition state equilibrium constants for C_6H_8S oxidation ($K^{\ddagger}_{Ox}$) as a function of inverse temperature on Ti-BEA (blue ▼, 3 mM C_8H_8, 0.01 M H_2O_2), Nb-BEA (black ■, 3 mM C_8H_8, 1 mM H_2O_2), Ta-BEA (orange ♦, 3 mM, 1 mM H_2O_2), and Zr-BEA (red ●) in CH_3CN. Dashed lines represent fits to the Eyring equation whose slopes are proportional to $\Delta H^{\ddagger}$.

References:

[1] R.J. Madon, M. Boudart, Experimental Criterion for the Absence of Artifacts in the Measurement of Rates of Heterogeneous Catalytic Reactions, Ind. Eng. Chem. Fundam., 21 (1982) 438-447.

[2] I. Chorkendorff, J.W.H. Niemantsverdriet, Concepts of Modern Catalysis and Kinetics, 2nd ed., Wiley-VCH Verlag Gmbh & Co., Weinheim, 2007.